Optimum Scanning Protocol for FDG-PET Evaluation of Pulmonary Malignancy

Val J. Lowe, David M. DeLong, John M. Hoffman and R. Edward Coleman

Division of Nuclear Medicine, Department of Medicine, Saint Louis University Medical Center, St. Louis, Missouri; Section of Nuclear Medicine, Department of Radiology, Duke University Medical Center, Durham, North Carolina; and Department of Neurology, Emory University, Atlanta, Georgia

FDG-PET can differentiate benign from malignant focal pulmonary opacities. We performed dynamic FDG-PET studies to determine the optimum time for emission data acquisition. **Methods:** Patients with focal pulmonary abnormalities demonstrated by biopsy to be malignant (n = 10) or benign (n = 4) were evaluated with dynamic FDG-PET. Dynamic PET data were acquired as sequential 5-min images for 2.5 hr. Radioactivity concentration measurements of the focal abnormality, a similar area in the opposite lung, and both lungs in the field of view were made throughout the period of acquisition. Standardized uptake ratios (SUR) of the lesions were calculated. SUR data and lesion-to-background ratios were plotted. The time that the SUR provided the maximum separation between benign and malignant masses after FDG administration was determined. **Results:** The SUR values provided the greatest separation between benign and malignant abnormalities beginning at 50 min and no advantage was identified in imaging later. Achievement of a 4:1 lesion-to-background ratio occurred by 50 min in malignant lesions. **Conclusion:** The acquisition of the emission data used in the evaluation of pulmonary malignancy should begin approximately 50 min after FDG administration.

Key Words: positron emission tomography; fluorine-18-fluorodeoxyglucose; lung neoplasms

J Nucl Med 1995; 36:883–887

FDG-PET can accurately differentiate benign from malignant pulmonary abnormalities (1–3). Quantitative FDG-PET studies of bronchogenic carcinoma have shown increased glucose metabolism in bronchogenic carcinoma compared to normal lung (4). Quantitative glucose metabolism studies are difficult to perform clinically because they require arterial blood sampling and are time consuming. To assess the data obtained from FDG-PET, many clinical centers have utilized a standardized uptake ratio (SUR) or other normalized uptake ratio to describe the FDG uptake. However, these uptake ratios may vary after the injection of FDG if the concentration of FDG in the abnormalities

changes with time. Thus, the time course of the accumulation of FDG in pulmonary lesions needs to be known so that the appropriate image acquisition time after FDG administration can be determined.

SURs obtained from data acquired 30–50 min after FDG administration have been accurate in differentiating benign from malignant solitary opacities (1,3). However, some infectious processes have SURs in the range that are considered positive for malignancy (1,3). Recent in vivo work has demonstrated that inflammatory cells have more rapid early uptake of FDG than do malignant cells, and this difference in early uptake may allow the differentiation of infectious and malignant lesions (5). Dynamic imaging of these processes is required to determine if any such benefit can be identified clinically.

Visual analysis of FDG-PET images of pulmonary nodules and opacities is accurate in the differentiation of benign and malignant processes (6). Maximizing target-to-background ratios is essential if physicians are to depend on visual evaluation of abnormalities from FDG-PET images and accurately identify regions of interest (ROIs) for semiquantitative analysis.

Therefore, patients with focal pulmonary abnormalities were studied using dynamic FDG-PET acquisitions to determine the kinetics of FDG accumulation in benign and malignant pulmonary abnormalities.

METHODS

Patients

Fourteen patients from our institution with indeterminate focal pulmonary abnormalities (not characterized as definitely benign or malignant by chest radiograph or CT scanning) were referred for evaluation by FDG-PET imaging and were entered in this protocol. All patients had definitive tissue diagnosis. To be eligible for the protocol, patients had to be willing and able to lie on the tomographic gantry for at least 3 hr. PET imaging of these patients was approved by the institutional review board of our hospital and informed consent was obtained. All patients fasted 4 hr prior to the PET study. One patient was an insulin-dependent diabetic. Blood glucose values at the time of the PET study were obtained on all patients.

PET Imaging

FDG-PET imaging was performed on either a GE 4096 Plus or Advance tomograph (GE Medical Systems, Milwaukee, WI). The

GE 4096 Plus produces 6.5-mm thick image planes (8 direct planes and 7 cross-planes). FWHM is 5 mm and the axial field of view is 10.3 cm. The Advance tomograph produces 4.25-mm thick image planes (18 direct planes and 17 cross planes). The axial field of view is 15 cm and the FWHM is 5 mm.

The ^{18}F-fluoride is produced by a CS-30 cyclotron (CTI, Berkeley, CA) facility. The ^{18}F-fluoride ions are transferred to either a CTI-Berkeley or General Electric automated system for synthesis of [^{18}F]2-deoxy-2-fluoro-D-glucose (FDG). FDG was tested for sterility, pyrogenicity, and radiochemical purity on each production run.

Patients were placed in the scanner so that the ROI was approximately in the center of the field of view of the scanner. The landmarks for positioning were determined from the chest radiograph and CT scan. Transmission scans using a rotating germanium-68 pin source were performed on all patients prior to injection of FDG. Emission images were obtained every 5 min after intravenous injection of 10.0 mCi of FDG and were acquired for 2.5 hr.

Transmission images were reconstructed using filtered backprojection and smoothed with a Hann window of 7.0 mm width. Emission images were reconstructed using filtered back-projection with a 5.0-mm wide Hann window. Emission data were corrected for scatter, random events and deadtime. Image pixel size was 3.0 mm in a 128 × 128 array.

Data Analysis

ROIs were placed over the focal abnormality on the PET study that corresponded to the abnormality on chest CT, an area of contralateral homologous normal lung parenchyma, and the entire lungs in the field of view. The chest radiograph and chest CT demonstrated no evidence of pathology in the lung that did not have the opacity. ROIs were placed in a summed 30–50-min acquisition image and copied to all images. Activity on each of the 5-min serial images was measured for each of the ROIs. For each patient SURs were calculated for the focal abnormalities in each of the serial 5-min emission frames according to the following formula:

$$\text{SUR} = \frac{\text{decay corrected mean ROI activity (mCi/ml)}}{\text{injected dose (mCi)/body wt (g)}}. \quad \text{Eq. 1}$$

Lesion-to-background ratios were calculated. Background activity was considered to be the average activity of the entire contralateral lung. The SUR values and lesion-to-background ratios were plotted against time after FDG administration. Maximal separation of benign and malignant mean SUR values was determined by calculating signal-to-noise ratio (SNR) measurements of log(SUR) for malignant and true negative benign mean SUR values. The log(SUR) values were used as the SNR is most appropriate for normally distributed data and they appeared to approximate a normal distribution better than the SUR values. Patient 945 was diabetic and had a serum glucose of 272 mg%. This patient was therefore excluded from the calculation. The signal-to-noise ratio for log(SUR) is estimated by means of the following. For each patient, 5-min averages of log(SUR) were computed, denote this value by $X_{i,j}$ for the i-th malignant patient and the j-th time interval and by $Y_{i,j}$ for the i-th benign patient and the j-th time interval. Then the signal-to-noise ratio (SNR) for the j-th time interval is estimated by:

$$\text{SNR} = (\bar{X}_j - \bar{Y}_j)/\sqrt{2\sigma_j^2}, \quad \text{Eq. 2}$$

where

$$\bar{X}_j = \sum_i X_{i,j}/n,$$
$$\bar{Y}_j = \sum_i Y_{i,j}/m, \quad \text{Eq. 3}$$

and

$$\sigma_j^2 = \left(\sum_i (X_{i,j} - \bar{X}_j)^2 + \sum_i (Y_{i,j} - \bar{Y}_j)^2 \right) \Big/ (n + m - 2) \quad \text{Eq. 4}$$

where n and m are the number of malignant and benign patients.

The SNR was thereby computed as the ratio of the difference in means (malignant group mean − benign group mean) divided by the pooled estimate of the standard deviation within each group. These SNR values were then plotted together with a fit generated by means of a cubic smoothing spline. Patient 129 was removed from the benign SUR mean calculation since its uptake was representative of a false-positive lesion (infection).

RESULTS

Ten patients had malignant disease: one large-cell undifferentiated tumor (Patient 729), one small-cell cancer (Patient 101), one mesothelioma (Patient 771), four well-differentiated adenocarcinomas (Patients 749, 758, 762 and 798), one poorly differentiated large-cell carcinoma (Patient 945), one moderately differentiated mucinous adenocarcinoma (Patient 757) and one poorly differentiated carcinoma (Patient 929). Four patients had benign lesions: one aspergillosis infection (Patient 129), one coccidiomycosis infection (Patient 849), one sarcoidosis (Patient 752) and one stable nodule for 8 yr (Patient 947). The SUR values were determined for each of the lesions and are shown in Figure 1. The SUR values provided the greatest separation (greatest SNR) between benign and malignant abnormalities beginning at about 50 min and no advantage was identified in imaging later (Fig. 2). Some point estimates of the pooled standard deviations in the malignant and benign groups are given in Table 1.

By evaluating dynamic uptake curves and specifically early uptake of FDG, no distinguishing characteristics between the 10 malignant and 2 infectious abnormalities (aspergillosis and coccidiomycosis) could be identified. Figure 1 shows the comparison of uptake in benign lesions with malignant lesions. A 4:1 lesion-to-background ratio occurred by 50 min in malignant lesions (Fig. 3A). The maximum lesion-to-background ratio in the benign group by 50 min was 9.5 for Patient AC00129. This study would represent a false-positive. With Patient AC00129 removed, the maximum lesion-to-background ratio in the benign group by 50 min was 2.4 (Fig. 3B). Figure 4 shows lesion, opposite lung control and both lung activity dynamic measurements during one study where a 6:1 lesion-to-background ratio was reached within 35 min of injection. Figure 5 shows the difference in contrast when emission data is acquired at 30 and 60 min.

DISCUSSION

FDG-PET can differentiate benign and malignant focal pulmonary opacities noninvasively (1,3). Protocols have
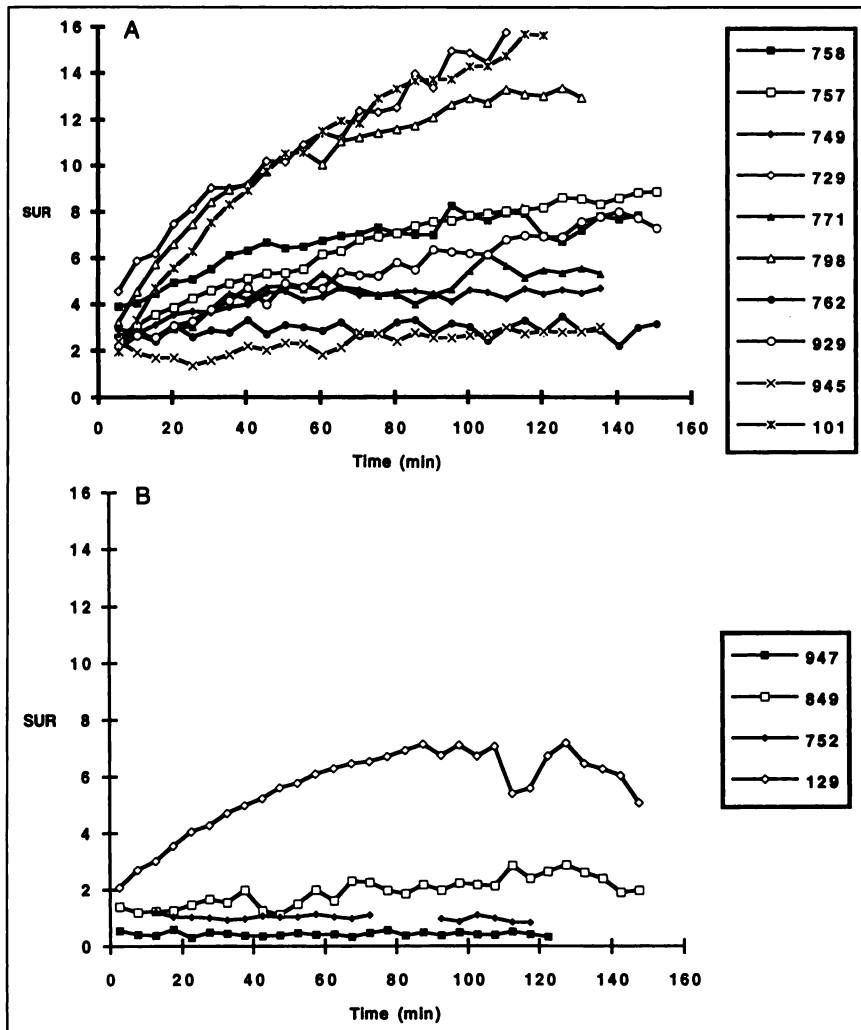
FIGURE 1. Plot of SUR of malignant (A) and benign (B) lesions against time. Large variations at later time points are due to patient movement (e.g., Patient 129).

Figure 1 legends:
A: 758, 757, 749, 729, 771, 798, 762, 929, 945, 101
B: 947, 849, 752, 129

varied in the timing of emission scan acquisition. SUR values will differ depending on the time at which the emission data are acquired, and this difference in timing of the acquisition makes comparison of data between institutions difficult. We performed serial 5-min images over 2.5 hr in patients with focal pulmonary opacities to determine the

optimal time to perform emission scans to identify malignancy. The time at which the SUR values provided maximal information during the dynamic acquisition was evaluated.

In the 14 patients we studied, 10 had documented malignancies and 4 had infectious or benign processes. We found that the optimum emission acquisition time was 50–60 min after injection of FDG. This time provides the shortest
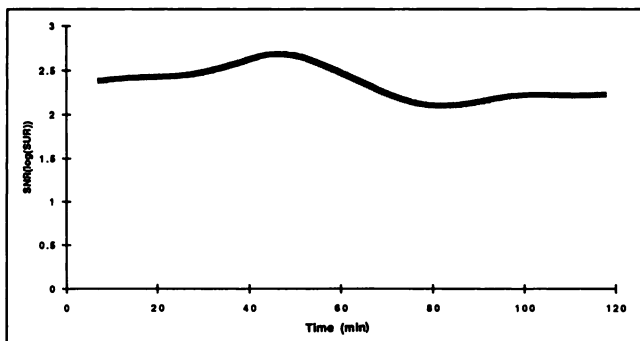
FIGURE 2. Plot of signal-to-noise ratio (SNR) of log(SUR) versus time showing increasing discrimination of malignant and benign lesions by SUR that peaks at about 50 min. A decline after that point represents increased noise from patient movement.

TABLE 1
Point Estimates of the Pooled Standard Deviations in the Benign and Malignant Groups

Time (min)	Malignant (s.d.)	Benign (s.d.)
12.5	0.31	0.69
27.5	0.45	0.61
42.5	0.43	0.70
57.5	0.50	0.80
72.5	0.56	0.80
87.5	0.57	1.07
102.5	0.58	0.84
112.5	0.60	0.89
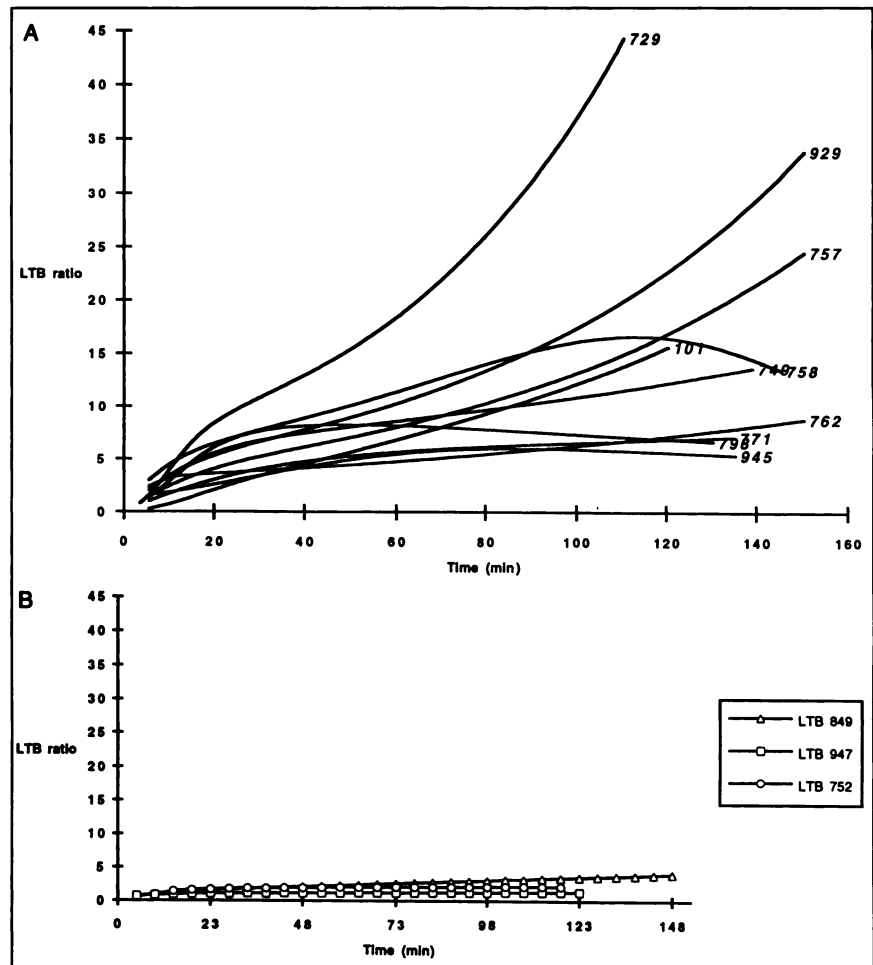
FIGURE 3. Plot against time of lesion-to-background (LTB) ratios for malignant (A) and benign (B) lesions.

waiting period at which maximal separation between malignant and benign lesions could be obtained by SUR data. The plot of signal-to-noise ratio (SNR) of log(SUR) shows that discrimination by SUR increased until about 50 min (Fig. 2). After that time there is some decline in discrimination because of noise induced by patient motion (some patients were seen to move on some frames as the studies progressed). Movement during the 2.5-hr study is unavoidable and we chose not to alter the ROI placement so as to prevent introduction of a second variable. Uptake in some of the tumors continued to increase during the 2.5 hr of the acquisition while others reached uptake plateaus.

No particular cell type accounted for the tumors with the

highest, steadily increasing uptake. This same finding was described by Nolop et al. (4). The initial uptake and peaks (Fig. 1A) were higher for three tumor types (small-cell in Patient 101, large-cell undifferentiated tumor in Patient 729, and well-differentiated adenocarcinoma in Patient 798). Poorly differentiated carcinoma in Patient 929 and well differentiated adenocarcinoma in Patients 762 and 758 were also seen in the moderate uptake range. The uptake rates and peaks may relate to several factors including the actual tumor uptake and the concentration of inflammatory cells.

In mice tumor models, Kubota et al. (5) showed that the uptake of FDG in macrophages associated with tumors was 2–4 times the uptake of the tumors (mammary carci-
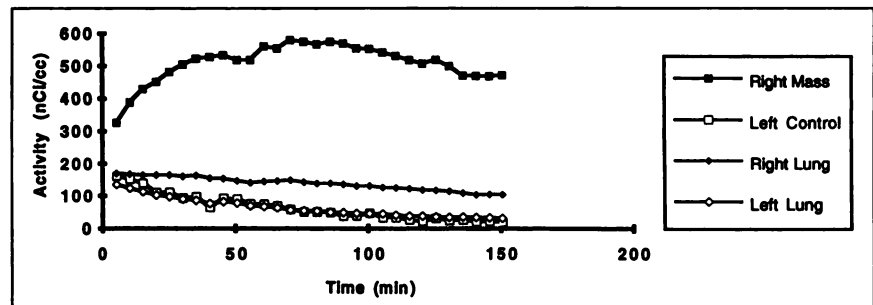
FIGURE 4. Plot of activity in a right lung moderately differentiated mucinous adenocarcinoma, a left lung control area, and the entire right (including tumor) and left lungs.
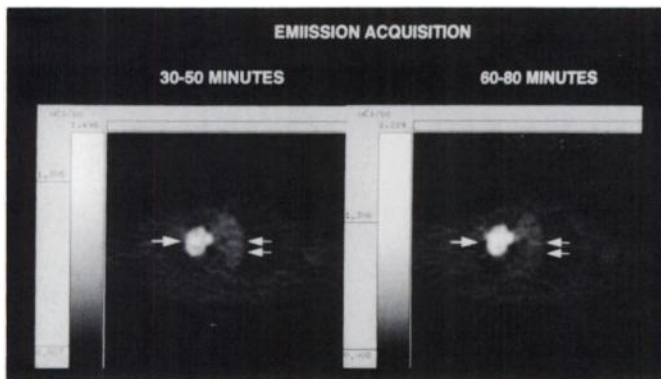
FIGURE 5. FDG-PET emission images of a malignant lesion (arrow) when data were summed from 30 to 50 min (LTB ratio of 12) and then at 60 min (LTB ratio of 15). Notice the decrease in blood-pool activity as seen in the aortic arch (arrows).

noma and hepatoma tumor models). They postulated that more rapid early uptake of FDG in the macrophages may allow differentiation of infectious and malignant lesions. The results of our study in humans do not confirm this postulate. In the limited number of patients that we evaluated, there were clearly three tumors that had higher and more rapid uptake than the infectious process that had the greatest amount of FDG accumulation of the infectious processes that we imaged. We could not visually identify any specific uptake characteristics of the high-grade infectious lesion from the uptake plots that would allow it to be differentiated from the malignant lesions (Fig. 1).

In one of the malignant cases, the SUR did not reach 2.5 by 50 min, but did by 80 min (Patient 945). We have demonstrated that an SUR value of 2.5 is accurate in differentiating benign and malignant lesions (3). This particular patient was diabetic, had a serum glucose of 272 mg% and therefore, may have had slower FDG uptake. This patient was therefore excluded from the SNR calculation. We are not certain if this patient received insulin prior to the PET study. Langen et al. (7) have shown that diminished tumor FDG uptake can occur with high serum glucose levels when imaged at 60 min. In all of the other patients, the highest glucose value was 165 mg% (Patient 771).

Lesion-to-background (LTB) ratios were obtained because visual evaluation of PET images is important (6), and maximizing the LTB ratio would aid in identifying abnor-

malities. All of the malignant lesions had reached a 4:1 LTB ratio by 60 min. Many had LTB ratios that were much higher. The hypometabolic benign group had a LTB ratio of 2.4 at 50 min. To evaluate the accuracy of different LTB ratios in detecting lesions of many different sizes with PET, a receiver-operator characteristic (ROC) study would need to be performed. However, this is beyond the scope of this investigation. Figure 5 shows the difference in contrast in an image that is acquired beginning at 30 min (LTB ratio of 12) and then at 60 min (LTB ratio of 15).

Appropriate acquisition times for other malignancies will need to be determined and the data in this study should not be extrapolated to other malignancies. Background activity will certainly differ depending on the location.

CONCLUSION

PET-FDG imaging of focal pulmonary abnormalities may produce different results if the emission acquisition periods vary after FDG administration. FDG continues to accumulate in many malignant and infection processes at least to a period of 2.5 hr, and this continuing accumulation results in variable SURs at different times in the uptake period. Imaging focal pulmonary abnormalities at approximately 50 min after FDG administration will produce optimum differentiation of benign and malignant lesions and provide target-to-background ratios that are at least 4:1 in malignant lesions.

REFERENCES

1. Gupta NC, Frank AR, Dewan NA, et al. Solitary pulmonary nodules: detection of malignancy with PET with 2-[F-18]-fluoro-2-deoxy-D-glucose. *Radiology* 1992;184:441–444.
2. Kubota K, Matsuzawa T, Fujiwara T, et al. Differential diagnosis of lung tumor with positron emission tomography: a prospective study. *J Nucl Med* 1990;31:1927–1932.
3. Patz EF, Lowe VJ, Hoffman JM, et al. Focal pulmonary abnormalities: evaluation with F-18 fluorodeoxyglucose PET scanning. *Radiology* 1993;188: 487–490.
4. Nolop KB, Rhodes CG, Brudin LH, et al. Glucose utilization in vivo by human pulmonary neoplasms. *Cancer* 1987;60:2682–2689.
5. Kubota R, Kubota K, Yamada S, Tada M, Ido T, Tamahashi N. Microautoradiographic study for the differentiation of intratumoral macrophages, granulation tissues and cancer cells by the dynamics of fluorine-18-fluorodeoxyglucose uptake. *J Nucl Med* 1994;35:104–112.
6. Lowe VJ, Hoffman JM, Patz EF, Paine S, Borrows P, Coleman RE. Differentiation of benign and malignant pulmonary opacities with FDG-PET [Abstract]. *J Nucl Med* 1993;34:21P.
7. Langen KJ, Braun U, Rota KE, et al. The influence of plasma glucose levels on fluorine-18-fluorodeoxyglucose uptake in bronchial carcinomas. *J Nucl Med* 1993;34:355–359.